PHYSICAL REVIEW B **81**, 060415(R) (2010)

Ultrafast three-dimensional magnetization precession and magnetic anisotropy of a photoexcited thin film of iron

E. Carpene,[1,*] E. Mancini,[1] D. Dazzi,[1] C. Dallera,[1] E. Puppin,[2] and S. De Silvestri[1]
[1]*CNR-INFM Ultras, Dipartimento di Fisica, Politecnico di Milano, Piazza Leonardo da Vinci 32, 20133 Milano, Italy*
[2]*CNISM, Dipartimento di Fisica, Politecnico di Milano, Piazza Leonardo da Vinci 32, 20133 Milano, Italy*
(Received 26 January 2010; revised manuscript received 5 February 2010; published 26 February 2010)

We investigated the three-dimensional dynamics of the magnetization vector launched by an intense infrared pulse of femtosecond duration in a thin Fe film. We demonstrate how a single experiment of time-resolved magneto-optical Kerr effect can provide quantitative information on the temporal evolution of the magnetization trajectory. Our approach allows us to follow the precessional motion of the magnetization and to retrieve the modulus and orientation of the magnetocrystalline anisotropy field as a function of time—and therefore of the local temperature—providing a direct experimental evidence of the phenomenological mechanism triggering the magnetization precession.

DOI: 10.1103/PhysRevB.81.060415 PACS number(s): 75.70.−i, 78.20.Ls, 78.47.−p, 78.66.Bz

A free magnetic moment misaligned with respect to a magnetic field undergoes a precessional motion known as Larmor precession. This motion is due to the torque the field exerts on **M** and it originates from its intrinsic angular momentum.[1] The period of the precession depends on the intensity of the field and lies in the picosecond regime for magnetic fields of the order of a tesla. This time scale attracts technological interest on ferromagnetic materials since the precession mechanism might provide a possible way to switch the magnetization, enhancing the speed of magnetic recording devices.[2] The precessional motion can be triggered by an ultrashort magnetic field pulse that misaligns the magnetization vector from its equilibrium position initiating the precession[3,4] or by an ultrashort and intense laser pulse acting as a heat source in metals[5,6] or inducing carrier excitations in magnetic semiconductors[7] or electronic transfer in garnets[8] that modify the magnetic anisotropy, thus leading to a rapid reorientation of the magnetization. The influence of the anisotropy on the magnetization dynamics has been reproduced with numerical simulations and compared to the measured data,[9–11] but a direct experimental proof of the mechanism is missing. We have set up a time-resolved magneto-optical Kerr effect (MOKE) experimental configuration that, without modifying neither the sample position nor the detection geometry, allows us to retrieve quantitative subpicosecond information about modulus and orientation of the magnetization in an epitaxial iron film, following an intense infrared laser pulse. As it will be shown, the magnetization vector undergoes a precessional motion triggered by the rapid change in the magnetocrystalline anisotropy. Our quantitative approach allows us to determine the heat-induced dynamics of the anisotropy field and provides the direct experimental evidence of the mechanism that launches the precession.

The experiment was carried out at room temperature on a thin Fe(001) film (about 8 nm thick) epitaxially grown on MgO(001). The magnetic layer is characterized by two easy axes along the [100] and the [010] directions and by a strong shape anisotropy that forces the magnetization to lie on the film plane. The optical analysis has been performed with an amplified Ti:Sapphire laser, generating 50 fs pulses centered at 800 nm (1.55 eV). The time resolution was achieved via the pump-probe technique (details can be found in Ref. 12). The *p*-polarized pump beam is focused on a spot size of about 200 μm with average fluence of 3 $\mathrm{mJ/cm^2}$. The incident, *p*-polarized probe beam hits the sample at an angle $\theta_i \simeq 47°$ with respect to the surface normal [Fig. 1(A)] and its spot size is about 70 μm. The external magnetic field $\mathbf{H}_{ext}$ is applied normal to the incidence plane and parallel to the sample surface. Before detection, the probe beam reflected from the sample passes through an analyzer oriented at an angle θ_a from the plane of incidence. The beam intensity I after the analyzer, normalized to the incident intensity, can be written as[13,14]

$$I(\theta_a) = (A + Bm_t)\cos^2\theta_a + (Cm_l + Dm_p)\cos\theta_a \sin\theta_a, \tag{1}$$

where A, B, C, and D are real coefficients depending on the complex refractive index, the magneto-optical constant of the material and the incidence angle θ_i, while $m_t = M_t/M_s$, $m_l = M_l/M_s$, and $m_p = M_p/M_s$ are the transverse (parallel to the external field), longitudinal (parallel to the sample and

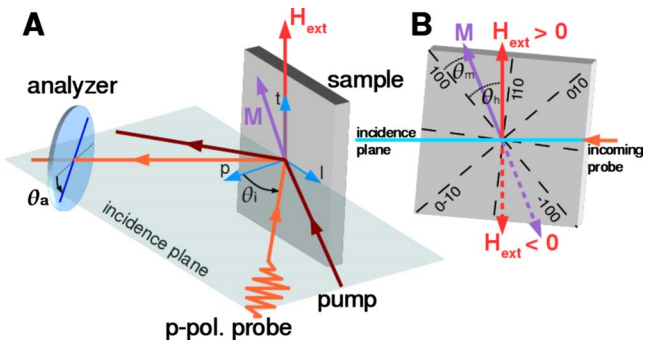

FIG. 1. (Color online) (a) Experimental geometry: the *p*-polarized pump and probe beams lie on the same incidence plane. The external magnetic field $\mathbf{H}_{ext}$ is applied along the sample surface and normal to the incidence plane. (b) External field $\mathbf{H}_{ext}$ and magnetization **M** form the angles θ_h and θ_m, respectively, with the [100] easy axis of the epitaxial Fe(001) film.

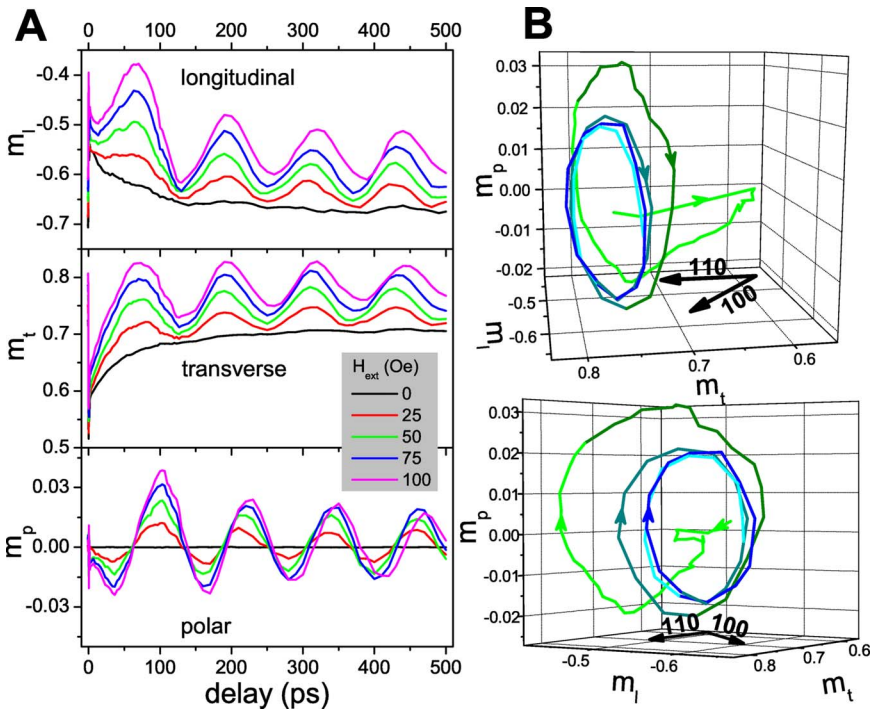

FIG. 2. (Color online) (a) Longitudinal, transverse, and polar (top to bottom) components of the magnetization vector vs pump-probe delay for different values of the external field (ranging from 0 to 100 Oe). (b) Two different views of the same real-space trajectory of the vector **M** (for H_{ext}=75 Oe). Various portions of the trajectory have been marked with different colors to ease the visualization.

normal to the field) and polar (normal to the sample) components, respectively, normalized to the saturation magnetization M_s. The θ_a dependence of the beam intensity in Eq. (1) suggests a way to separate the different components: by measuring I at two opposite orientation of the analyzer, it is easily shown that (for θ_a=45°) $I_p=I(\theta_a)+I(-\theta_a)=A+Bm_t$, while $I_n=I(\theta_a)-I(-\theta_a)=Cm_l+Dm_p$.[15] The measurement of I_p allows us to access m_t, but in order to fully determine **M**, we must isolate m_l from m_p in the expression of I_n. According to the Fresnel formulation, the coefficient C is an odd function of the incidence angle θ_i, while D is even.[14] To separate m_l from m_p, one should therefore measure I_n for opposite incidence angles and perform sums and differences. However, the same result can be obtained exploiting the cubic symmetry of the iron sample without modifying the experimental setup. Referring to Fig. 1(B), it is easily seen that inverting the incidence angle θ_i is equivalent to inverting the applied magnetic field (dashed lines). Therefore, taking the intensity $I_n(H_{ext})$ at opposite external field we can write $I_n(\pm H_{ext})=(\pm Cm_l+Dm_p)$ that allows us to separate the longitudinal from the polar projection.

The technique described above has been exploited to investigate the precessional motion of the magnetization vector triggered by a short intense laser pulse. Starting with the magnetization along the [+100] ([−100]) direction, a static positive (negative) external field not aligned to an easy axis changes the orientation of **M** toward the field (this is known as *coherent rotation*[16]). In order to maximize this effect, in our experiment the angle between the external field and the easy axis has been set to $\theta_h \approx 44°$ [see Fig. 1(B)]. Under such conditions, the magnetization precession triggered by a laser pulse can be easily observed. Figure 2(A) reports the components m_l, m_t, and m_p as a function of the pump-probe delay for five different intensities of the external field, ranging from 0 to 100 Oe. Without external field, no oscillation and no polar component are present (black lines): the modulus of the magnetization vector rapidly drops of about 30% at 0 ps delay and then slowly recovers within a few hundreds of picoseconds. In the presence of external field, the oscillatory behavior becomes clearly visible, with a period of roughly 120 ps, while the amplitude of the oscillations increases with the field intensity. The polar component is phase shifted by $\pi/2$ relative to the longitudinal and transverse magnetization (parallel to the film), indicating a precessional motion. It should be noticed that the frequency of the oscillations slightly decreases with increasing external field. Although this phenomenon seems to contradict the Larmor theorem, it is a consequence of the biaxial nature of the magnetocrystalline anisotropy in the Fe film and it can be properly explained.[11] The three-dimensional (3D) trajectory of the magnetization is reconstructed in Fig. 2(B) (the two panels report the same plot from different views). The initial drop of the magnetization (within a few hundreds of fs) takes place only on the film plane, while the subsequent recovery is characterized by well discernible out-of-plane components. The amplitude of the coils reduces, while their center shifts toward the [100] crystallographic direction as the system relaxes back to equilibrium. The amplitude of the in-plane oscillations is about 4–5 times larger than those of the out-of-plane polar component. This is caused by the shape anisotropy effects that forces the magnetization to lie preferentially on the film plane.

Having discussed the qualitative features of the oscillations, we now seek their interpretation. We begin with some

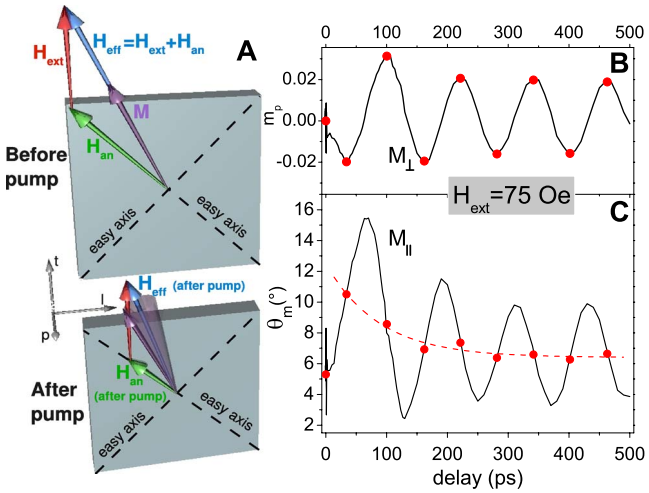

FIG. 3. (Color online) (a) Schematic diagram of the angular relation between $\mathbf{M}$ and the effective field ($\mathbf{H}_{ext}+\mathbf{H}_{an}$) in static condition (top) and after the laser pumping (bottom). (b) Projection of the magnetization trajectory (for $H_{ext}=75$ Oe) normal to the surface and (c) evolution of the in-plane orientation of $\mathbf{M}$ relative to the [100] easy axis. The dashed line represents the in-plane angular position of the precession axis (see text).

basic consideration on the static case. As shown in Fig. 1(B), θ_m and θ_h are the angles (on the film plane) made by the magnetization $\mathbf{M}$ and the external field $\mathbf{H}_{ext}$, respectively, with the [100] easy axis. If $\mathbf{H}_{ext}=0$, the magnetization lies along the easy axis, i.e., $\theta_m=0$. In the presence of an external field $\mathbf{H}_{ext}$ parallel to the magnetic layer but not aligned to an easy axis, the orientation θ_m of the magnetization vector can be deduced by minimizing the in-plane free-energy density g (in dimensionless form) of a thin film with biaxial magnetocrystalline anisotropy:[17]

$$g = \frac{1}{8}\sin^2 2\theta_m - \frac{H_{ext}}{H_{an}}\cos(\theta_m - \theta_h), \tag{2}$$

where $H_{an}=2K_1/\mu_0 M_s$ is the intensity of the so-called anisotropy field lying along the easy axis [for bulk iron $H_{an}=550$ Oe (Ref. 13)] and K_1 is the magnetocrystalline anisotropy constant. It can be shown that for a small angle θ_m, the quantity g is equivalent to the energy term $-\mu_0\mathbf{M}\cdot(\mathbf{H}_{ext}+\mathbf{H}_{an})$. This means that in the presence of an external field, the magnetization $\mathbf{M}$ aligns with the effective field given by the vector sum $\mathbf{H}_{eff}=\mathbf{H}_{ext}+\mathbf{H}_{an}$ [top panel of Fig. 3(A)].

But what happens when the sample is irradiated by a short and intense laser pulse? The effect of the irradiation is to locally heat the sample, increasing the temperature of the irradiated volume. The local thermal equilibrium is established within a few picoseconds, a time scale comparable to the electron-lattice relaxation time.[12] During this time, the saturation magnetization M_s and the magnetocrystalline anisotropy constant K_1, both depending on the temperature, will decrease. K_1 has a stronger temperature dependence compared to M_s,[18] therefore the intensity of the anisotropy field $H_{an}\propto K_1/M_s$ will drop. Since the external field is unaffected, the total effective field will decrease and rotate toward $\mathbf{H}_{ext}$. The magnetization vector will no longer be aligned to the effective field and it will experience a torque that launches the precessional motion around the time-dependent field $\mathbf{H}_{eff}(t)$ [see lower panel of Fig. 3(A)]. This motion is described by the well-known Landau-Lifshitz-Gilbert (LLG) equation,[19] according to which the vector $\mathbf{M}$ precesses around the effective field and experiences a dissipative damping that hampers the oscillations. Eventually, the magnetization will align along $\mathbf{H}_{eff}$ that represents the axis of the precessional cone. In our case, the effective field is time (i.e., temperature) dependent and its modulus and orientation can be retrieved from the magnetization trajectory and from Eq. (2) with the following argument: if one could *freeze* the effective field at a certain delay τ after the pump, the magnetization vector would precess around $\mathbf{H}_{eff}(\tau)$ and ultimately, owing to the damping, align along it. Due to the geometry of our experiment, the precession axis always lies on the film plane. Thus, the final equilibrium magnetization would also be in plane and its orientation θ_m would be the one minimizing Eq. (2). Since θ_h and H_{ext} are fixed experimental parameters, the orientation θ_m would unequivocally determine $H_{an}(\tau)$. The analysis of the in-plane and out-of-plane dynamics of $\mathbf{M}$ gives access to the sought angle θ_m at different delays. Figure 3(B) reports the time evolution of the out-of-plane (i.e., polar) component of the magnetization vector, while panel C plots the time evolution of the angle θ_m between the in-plane projection of the magnetization vector and the [100] easy axis. The red dots mark the points in time when the polar component of the magnetization has a maximum or a minimum. According to the elementary property of a precessional motion, at those points the in-plane component of $\mathbf{M}$ is aligned with the precession axis [large dots in Fig. 3(C)], and the corresponding values of the angles θ_m inserted in Eq. (2) provide the time dependence of $H_{an}(t)$.

The result of this procedure is shown in Fig. 4(A) that reports the temporal evolution of the magnetocrystalline anisotropy field obtained independently from the three sets of data corresponding to applied fields H_{ext} of 50, 75, and 100 Oe. At negative delay (slightly before the pump hits the sample) the extrapolated values of H_{an} compare well with the anisotropy field of bulk iron (550 Oe), but a few tens of ps after pumping, H_{an} drops to about half of its initial value and slowly recovers within a few hundreds of ps. The time evolution of the anisotropy constant K_1 is obtained by inserting in the expression of H_{an} the temporal dependence of the magnetization M_s as deduced from the data shown in Fig. 2(A) without external field. Since the variation in the anisotropy constant is determined by the change in the local temperature T that is itself a function of the pump-probe delay, it is physically more significant to plot K_1 as a function of T. To achieve this, we must convert the time scale of Fig. 4(A) into a temperature scale. A simple way is provided directly by the experimental curve $M_s(t)$. For sufficiently long delay (a few picoseconds) after the pump, electrons, spins, and lattice have reached thermal equilibrium and the saturation magnetization is uniquely determined by the local temperature. In iron, the temperature dependence of $M_s(T)$ is well known and it can be analytically expressed as $M_s(T)/M_s(0)=(1-\eta)^b/(1-b\eta+a\eta^{3/2}-c\eta^{7/2})$, being $\eta=T/T_C$ ($T_C=1044$ K is the Curie temperature of Fe), $a=0.1098$, $b=0.368$, and $c=0.129$.[20] By numerically inverting

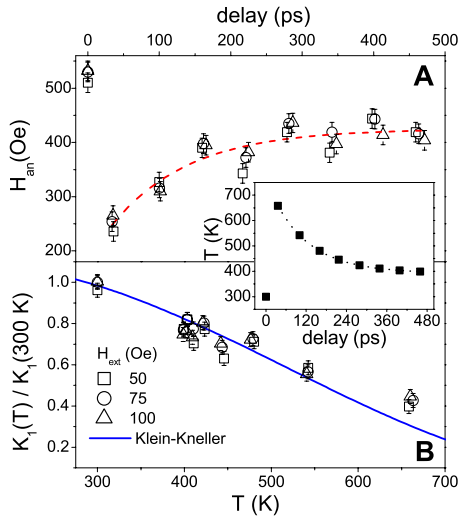

FIG. 4. (Color online) (a) Experimental evolution of the (in-plane) magnetocrystalline anisotropy field vs pump-probe delay (the dashed line is a guide for the eye). (b) Temperature dependence of the magnetocrystalline anisotropy constant (dots), normalized to its room-temperature value as obtained from the data (see text). The solid line is taken from Ref. 18 for comparison. The inset reports the time evolution of the local temperature T obtained from the magnetization data (see text).

this formula, the function $T(M_s)$ is obtained, and using the experimental values of $M_s(t)$, we end up with an empirical relation that allows us to convert the pump-probe delay into a temperature scale (inset to Fig. 4). The magnetocrystalline anisotropy constant K_1 deduced from our experiment as a function of the local temperature is compared in Fig. 4(B) to the original data of Ref. 18. The remarkable agreement strongly reinforces our interpretation and endorses the reliability of the experimental method. As a final remark, we point out that the field dependence of the precession frequency ω for this thin film with in-plane anisotropy is given by $\omega=\gamma g\sqrt{H_{eff}H_{dem}}$, with γ as the gyromagnetic ratio and $g\simeq 2$ as the Landé splitting.[21] $H_{dem}=\mu_0 M_s$ is the demagnetizing field normal to the sample surface. From the experimental values of the precession frequency and the effective field we obtain $H_{dem}\approx 2$ T that matches fairly well the iron bulk magnetization of 2.1 T.

In conclusion, we have presented the investigation of time-resolved MOKE performed in an experimental geometry that provides the full quantitative dynamics of both the magnetization vector **M** and the magnetocrystalline anisotropy. From the temporal evolution of **M** (modulus and orientation), the heat-induced dynamics of the anisotropy constant of iron has been retrieved. Our method provides the clear and direct experimental evidence of the mechanism that launches the magnetization precession, and in view of the flourishing interest on femtomagnetism,[22] it represents a simple and widely applicable way to study the ultrafast evolution of the spin order in magnetic structures.

Fondazione Cariplo is gratefully acknowledged for financial support.

*ettore.carpene@fisi.polimi.it

[1] L. D. Landau and E. M. Lifshitz, *Mechanics and Electrodynamics* (Pergamon, Oxford, 1972).
[2] I. Tudosa, C. Stamm, A. B. Kashuba, F. King, H. C. Siegmann, J. Stöhr, G. Ju, B. Lu, and D. Weller, Nature (London) **428**, 831 (2004).
[3] W. K. Hiebert, A. Stankiewicz, and M. R. Freeman, Phys. Rev. Lett. **79**, 1134 (1997).
[4] Y. Acremann, C. H. Back, M. Buess, O. Portmann, A. Vaterlaus, D. Pescia, and H. Melchior, Science **290**, 492 (2000).
[5] M. van Kampen, C. Jozsa, J. T. Kohlhepp, P. LeClair, L. Lagae, W. J. M. de Jonge, and B. Koopmans, Phys. Rev. Lett. **88**, 227201 (2002).
[6] Q. Zhang, A. V. Nurmikko, A. Anguelouch, G. Xiao, and A. Gupta, Phys. Rev. Lett. **89**, 177402 (2002).
[7] Y. Hashimoto, S. Kobayashi, and H. Munekata, Phys. Rev. Lett. **100**, 067202 (2008).
[8] F. Hansteen, A. Kimel, A. Kirilyuk, and T. Rasing, Phys. Rev. Lett. **95**, 047402 (2005).
[9] M. Vomir, L. H. F. Andrade, L. Guidoni, E. Beaurepaire, and J.-Y. Bigot, Phys. Rev. Lett. **94**, 237601 (2005).
[10] J.-Y. Bigot, M. Vomir, L. H. F. Andrade, and E. Beaurepaire, Chem. Phys. **318**, 137 (2005).
[11] H. B. Zhao, D. Talbayev, Q. G. Yang, G. Lüpke, A. T. Hanbicki, C. H. Li, O. M. J. van't Erve, G. Kioseoglou, and B. T. Jonker, Appl. Phys. Lett. **86**, 152512 (2005).
[12] E. Carpene, E. Mancini, C. Dallera, M. Brenna, E. Puppin, and S. De Silvestri, Phys. Rev. B **78**, 174422 (2008).
[13] J. M. Florczak and E. D. Dahlberg, Phys. Rev. B **44**, 9338 (1991).
[14] Z. J. Yang and M. R. Scheinfein, J. Appl. Phys. **74**, 6810 (1993).
[15] The full hysteresis loop is measured for each pump-probe delay, i.e., at each chosen delay, the beam intensity is recorded sweeping the external field between −100 and +100 Oe for the two orientations of the analyzer. This allows us to easily separate the field-dependent term in I_p from the coefficient A. The coefficients B and C (in particular their ratio) have been experimentally deduced in static conditions (i.e., without pump and thus with $m_p=0$) measuring the longitudinal and transverse components of **M**, saturated along a given easy axis, for various orientations of the sample (i.e., various θ_m) and using the fact that $m_t^2+m_l^2=1$. The coefficient D has been estimated using the optical and magneto-optical coefficients of iron available in the literature. Due to the variety of data, its value might be correct within a factor of two.
[16] E. C. Stoner and E. P. Wohlfarth, Philos. Trans. R. Soc. London, Ser. A **240**, 599 (1948).
[17] G. Bertotti, *Hysteresis in Magnetism* (Academic Press, San Diego, 1998), Chap. 8, p. 235.
[18] H.-P. Klein and E. Kneller, Phys. Rev. **144**, 372 (1966).
[19] T. L. Gilbert, IEEE Trans. Magn. **40**, 3443 (2004).
[20] S. D. Hanham, A. S. Arrott, and B. Heinrich, J. Appl. Phys. **52**, 1941 (1981).
[21] C. Kittel, Phys. Rev. **73**, 155 (1948).
[22] G. P. Zhang, W. Hübner, G. Lefkidis, Y. Bai, and T. F. George, Nat. Phys. **5**, 499 (2009); J.-Y. Bigot, M. Vomir, and E. Beaurepaire, *ibid.* **5**, 515 (2009).